

## Critical Current of SF–NFS Josephson Junctions

I. I. Soloviev<sup>a, b, \*</sup>, N. V. Klenov<sup>b, c</sup>, S. V. Bakursky<sup>c–e</sup>,  
M. Yu. Kupriyanov<sup>a, d, f</sup>, and A. A. Golubov<sup>d, e</sup>

<sup>a</sup> Skobeltsyn Institute of Nuclear Physics, Moscow State University, Moscow, 119991 Russia  
\*e-mail: isol@phys.msu.ru

<sup>b</sup> Lukin Research Institute for Physical Problems, Zelenograd, Moscow, 124460 Russia

<sup>c</sup> Faculty of Physics, Moscow State University, Moscow, 119991 Russia

<sup>d</sup> Moscow Institute of Physics and Technology (State University),  
Institutskii per. 9, Dolgoprudnyi, Moscow region, 141700 Russia

<sup>e</sup> Faculty of Science and Technology and MESA, Institute for Nanotechnology, University of Twente,  
7500 AE Enschede, Netherlands

<sup>f</sup> Institute of Physics, Kazan (Volga region) Federal University, Kremlevskaya ul. 18, Kazan, 420008 Russia  
Received December 9, 2014

The properties of SF–NFS sandwiches composed of two superconducting (S) electrodes separated by a weak-link region formed by a normal-metal (N) step with the thickness  $d_N$  situated on the top of a lower S electrode and a ferromagnetic (F) layer with the thickness  $d_F$  deposited onto the step and the remaining free surface of the lower electrode have been studied theoretically. It has been shown in the approximation of linearized semiclassical Usadel equations that the two-dimensional problem in the weak-link region can be reduced to two one-dimensional problems in its SFS and SNFS segments. The spatial distributions of the critical current density  $J_c$  in the segments as a function of the layer thickness  $d_F$  have been calculated. The dependences of the critical current  $I_c$  of the structure on the magnitude of the magnetization vector  $\mathbf{M}$  of the ferromagnetic layer have been found for various directions of the magnetization within the junction plane. It has been shown that these dependences are affected considerably by both the orientation of  $\mathbf{M}$  and the spatial distribution of  $J_c$ .

DOI: 10.1134/S002136401504013X

Investigation of the processes in Josephson junctions composed of superconducting (S) and ferromagnetic (F) materials is of growing fundamental and applied interest. In particular, theoretical [1–3] and experimental [4–16] works showed that the critical current  $I_c$  of such structures depends on the mutual orientation of the magnetization vectors  $\mathbf{M}$  of the ferromagnetic films situated in the weak-link region. This effect can be used to create superconducting spin valves, which can be applied as control units of superconducting memory compatible with rapid single flux quantum (RSFQ) logic [17].

However, experimental works [7–16] showed that the typical voltages  $V_c = I_c R_n$  across the valves (where  $R_n$  is the normal resistance of the junction) containing two or more F films in the weak-link region lie in the microvolt and nanovolt ranges, respectively. These values are several orders of magnitude lower than  $V_c$  of junctions used in RSFQ circuits. Strong suppression of  $I_c$  has a simple physical nature: to accomplish the control effect, one has to remagnetize one of the F layers without changing the direction of  $\mathbf{M}$  in the other F film. This can be only done if the weak link is a combination of “strong” and “weak” ferromagnets, i.e., the materials with considerably different exchange ener-

gies  $H$  and/or thicknesses of F layers. As a result,  $I_c$  is manipulated against the background of its considerable suppression by the strong ferromagnet. This hinders the use of such valves as control units of superconducting memory.

Superconductor–insulator–superconducting film–ferromagnetic metal–superconductor (SISFS) Josephson junctions proposed in [6, 18–21] and composed of a series of an SIs tunnel junction with a high characteristic voltage  $V_c$  and an sFS junction with one F layer, which allows switching this voltage  $V_c$  on and off by applying an external magnetic field  $H_{\text{ext}}$ , are free from the above drawback. However, their use in superconducting memory units encounters certain difficulties in performing read/write operations. These difficulties are associated with a possible drift of  $I_c$  at  $H_{\text{ext}} = 0$  that occurs in multiple information rewriting to the memory unit. The use of several ferromagnetic layers in the sFS part, e.g., switching to SISF<sub>1</sub>F<sub>2</sub>S or SISF<sub>1</sub>F<sub>2</sub>F<sub>3</sub>S junctions, eliminates the problem of  $I_c$  uncertainty at  $H_{\text{ext}} = 0$ . However, this solution imposes serious constraints on the critical current of the tunnel SIs part of the control element, which must be much

lower than  $I_c$  of the  $\text{SIsF}_1\text{F}_2\text{S}$  or  $\text{SIsF}_1\text{F}_2\text{F}_3\text{S}$  junctions at  $H_{\text{ext}} = 0$ .

In this work, we will show that a possible solution of the above contradiction is to create an artificial anisotropy in the weak-link region by introducing an inhomogeneity, the presence of which leads to the formation of regions with positive (0 contact) and negative ( $\pi$  contact) critical supercurrent densities inside the junction [22–27].

**Model of a SF–NFS Josephson junction.** We consider a layered structure shown in Fig. 1. It consists of superconducting electrodes separated by a ferromagnetic interlayer with the thickness  $d_F$  or by a sandwich containing the same F layer and a normal-metal (N) layer with the thickness  $d_N$ .

We will assume that the “dirty”-limit conditions are satisfied for all metals and that the effective electron–phonon coupling constant in the F and N materials is zero. For further simplification, we will assume that the temperature  $T$  is close to the critical temperature  $T_c$  of superconducting electrons. Under the above assumptions, the solution of the problem of computing the spatial distribution of the superconducting current density  $J_S$  in the structure of interest is reduced to the solution of the linearized Usadel equations [28]

$$\xi_N^2 \left\{ \frac{\partial^2}{\partial x^2} + \frac{\partial^2}{\partial y^2} \right\} F_N - \Omega F_N = 0, \quad (1)$$

$$\xi_F^2 \left\{ \frac{\partial^2}{\partial x^2} + \frac{\partial^2}{\partial y^2} \right\} F_F - \tilde{\Omega} F_F = 0, \quad (2)$$

$$\frac{2eJ_S(\varphi)}{\pi T \sigma_F} = i \sum_{\omega=-\infty}^{\infty} \left( F_{F,\omega} \frac{\partial F_{F,-\omega}^*}{\partial y} - F_{F,-\omega}^* \frac{\partial F_{F,\omega}}{\partial y} \right). \quad (3)$$

Here,  $\Omega = |\omega|/\pi T_c$ ;  $\tilde{\Omega} = (\Omega + ih\text{sgn}\omega)$ ;  $h = H/\pi T_c$ ;  $\xi_{N,F}^2 = (D_{N,F}/2\pi T_c)$ , where  $D_{N,F}$  are the diffusion coefficients;  $\omega = \pi T(2n + 1)$  are the Matsubara frequencies;  $H$  is the exchange energy in the ferromagnetic material;  $F_{N,F}$  are the Usadel Green’s functions in the normal and ferromagnetic films, respectively; and  $\varphi$  is the phase difference of the order parameters in the S electrodes. By writing Eqs. (1) and (2), we specified the directions of the  $x$  and  $y$  axes parallel and perpendicular to the SF interface and placed the origin at the SF interface (Fig. 1). The set of Eqs. (1) and (2) must be supplemented by the boundary conditions [29]. To write these conditions, we assume that the suppression parameter  $\gamma_{\text{BF}} = R_{\text{BF}} \mathcal{A}_{\text{BF}} / \rho_F \xi_F$  at the SF interface is large enough,

$$\gamma_{\text{BF}} \gg \max\{1, \rho_S \xi_S / \rho_F \xi_F\}, \quad (4)$$

to neglect superconductivity suppression in the superconducting electrodes. Here,  $R_{\text{BF}}$  and  $\mathcal{A}_{\text{BF}}$  are the

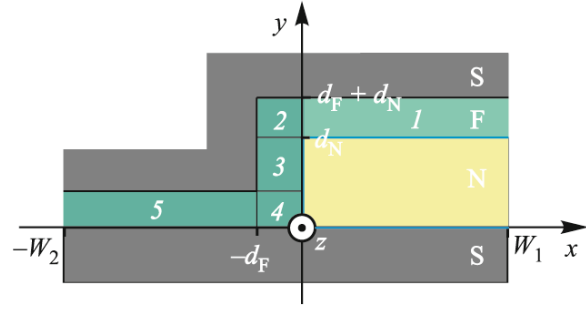


**Fig. 1.** (Color online) Scheme of a spatially inhomogeneous layered structure with a thin normal layer introduced into a part of the SF interface region.

resistance and area of the SF interface, respectively;  $\xi_S = (D_S/2\pi T_c)^{1/2}$  and  $\xi_F$  are the coherence lengths in the superconductors and ferromagnet, respectively;  $\rho_S$  and  $\rho_F$  are their resistivities; and  $D_S$  is the diffusion coefficient of the superconductor. In contrast, the SN and FN interfaces are thought to be transparent to electrons. Under the above assumptions, the boundary conditions [29] can be represented in the form

$$\frac{\partial F_S}{\partial y} = \frac{\gamma_S \xi_N}{\xi_S} \frac{\partial F_N}{\partial y}, \quad F_S = F_N, \quad y = 0, \quad (5a)$$

$$0 \leq x \leq W_1,$$

$$\frac{\partial F_N}{\partial y} = \frac{\gamma_N \xi_F}{\xi_N} \frac{\partial F_F}{\partial y}, \quad F_F = F_N, \quad y = d_N, \quad (5b)$$

$$0 \leq x \leq W_1,$$

$$\frac{\partial F_N}{\partial x} = \frac{\gamma_N \xi_F}{\xi_N} \frac{\partial F_F}{\partial x}, \quad F_F = F_N, \quad x = 0, \quad (5c)$$

$$0 \leq y \leq d_N,$$

$$\frac{\partial F_F}{\partial y} = \frac{\Delta \exp(-i\varphi/2)}{|\omega| \gamma_{\text{BF}} \xi_F}, \quad y = 0, \quad -W_2 \leq x \leq 0, \quad (5d)$$

$$\frac{\partial F_F}{\partial y} = -\frac{\Delta \exp(i\varphi/2)}{|\omega| \gamma_{\text{BF}} \xi_F}, \quad \begin{cases} y = d_F, & -W_2 \leq x \leq 0, \\ y = d_N + d_F, & 0 \leq x \leq W_1, \end{cases} \quad (5e)$$

$$\frac{\partial F_F}{\partial x} = -\frac{\Delta \exp(i\varphi/2)}{|\omega| \gamma_{\text{BF}} \xi_F}, \quad x = -d_F, \quad (5f)$$

$$d_F \leq y \leq d_N + d_F$$

$$\frac{\partial F_N}{\partial x} = 0, \quad x = W_1, \quad 0 \leq y \leq d_N, \quad (5g)$$

$$\frac{\partial F_F}{\partial x} = 0, \quad \begin{cases} x = W_1, & d_N \leq y \leq d_N + d_F, \\ x = -W_2, & 0 \leq y \leq d_F. \end{cases} \quad (5h)$$

Here,  $\Delta \exp(\pm i\varphi/2)$  is the order parameter in the upper and lower superconducting electrodes, respectively, and

$$\gamma_N = \frac{\rho_N \xi_N}{\rho_F \xi_F}, \quad \gamma_S = \frac{\rho_S \xi_S}{\rho_N \xi_N}. \quad (6)$$

In the typical experimental situation, superconductors are made of Nb ( $\rho_S \approx 7 \times 10^{-6} \Omega \text{ cm}$ ,  $\xi_S \approx 10 \text{ nm}$ ) and the normal metal is Cu ( $\rho_N \approx 10^{-6} \Omega \text{ cm}$ ,  $\xi_N \approx 100 \text{ nm}$ ). Setting  $\rho_F \approx 10^{-5} \Omega \text{ cm}$  and  $\xi_F \approx 10 \text{ nm}$ , we find relatively high suppression parameters  $\gamma_N \approx 1$  and  $\gamma_S \approx 0.7$  at the FN and SN interfaces.

To solve the boundary value problem given by Eqs. (1), (2), and (5a)–(5h), it is convenient to divide the ferromagnetic film into five segments (see Fig. 1) and, in the first approximation, to neglect the contributions to the function  $F_F$  from the angular segments denoted by the digits 2 and 4 in Fig. 1. Assuming further that the derivatives of the function  $F_F$  along the directions of the normal to the boundary between the angular segment and the other parts of the ferromagnetic layer vanish, the problem can be reduced to the solution of one-dimensional Eqs. (1) and (2) in the regions 1, 3, and 5.

The solution in the region 1 can be expressed as

$$F_F = \frac{\Delta \exp(i\varphi/2) \sinh[\sqrt{\Omega}(y - d_N)/\xi_F]}{|\omega| \sqrt{\Omega} \gamma_{BF} \cosh[\sqrt{\Omega} d_F/\xi_F]} + \frac{F_N(d_N) \cosh[\sqrt{\Omega}(y - d_N - d_F)/\xi_F]}{\cosh(\sqrt{\Omega} d_F/\xi_F)}, \quad (7)$$

where  $F_N(d_N)$  is the integration constant. It follows from Eqs. (1) and (7) that, in the region  $y = d_N$ ,  $0 \leq x \leq W_1$ ,

$$\xi_N \frac{\partial}{\partial y} F_N = \gamma_N \sqrt{\Omega} F_N(d_N) \tanh\left(\frac{\sqrt{\Omega} d_F}{\xi_F}\right) - \frac{\gamma_N \Delta \exp(i\varphi/2)}{|\omega| \gamma_{BF}} \frac{1}{\cosh(\sqrt{\Omega} d_F/\xi_F)}. \quad (8)$$

Typical thicknesses of the normal film lie in the range of  $d_N \lesssim 20 \text{ nm}$ , which is much less than  $\xi_N$ . In view of this circumstance, it is readily found from Eq. (8) that, if the inequalities  $\gamma_N \sqrt{h} d_N/\xi_N \ll 1$  and  $\gamma_N d_N/\gamma_{BF} \xi_N \ll 1$  hold, condition (8) is greatly simplified and in the first approximation with respect to these small parameters is reduced to the equality

$$\xi_N \frac{\partial}{\partial y} F_N = 0, \quad y = d_N, \quad 0 \leq x \leq W_1. \quad (9)$$

The solution of the boundary value problem specified by Eqs. (1), (2), and (5a)–(5h) in the region 3 can be expressed as

$$F_F(x) = F_N(0) \frac{\cosh[\sqrt{\Omega}(d_F - x)/\xi_F]}{\cosh(\sqrt{\Omega} d_F/\xi_F)} + \frac{\Delta \exp(i\varphi/2) \sinh(\sqrt{\Omega} x/\xi_F)}{|\omega| \sqrt{\Omega} \gamma_{BF} \cosh(\sqrt{\Omega} d_F/\xi_F)}, \quad (10)$$

and therefore

$$\xi_N \frac{\partial}{\partial x} F_N(0) = -\gamma_N \sqrt{\Omega} F_N(0) \tanh\left(\frac{\sqrt{\Omega} d_F}{\xi_F}\right) + \frac{\gamma_N \Delta \exp(i\varphi/2)}{|\omega| \gamma_{BF}} \frac{1}{\cosh(\sqrt{\Omega} d_F/\xi_F)}. \quad (11)$$

It follows from Eq. (11) that  $\gamma_N \sqrt{h} \gg 1$  at  $\sqrt{h} d_F \geq \xi_F$ . Since the derivative on the left-hand side of Eq. (11) at  $W_1 \gg \xi_N$  varies at a distance on the order of  $\xi_N$  so that  $\xi_N \partial F_N/\partial x \approx 1$ , condition (11) in the first approximation with respect to  $(\gamma_N \sqrt{h})^{-1} \ll 1$  is reduced to the boundary condition of the first kind:

$$F_N(0) = 0. \quad (12)$$

This condition holds at the entire FN interface located at  $x = 0$ .

At last, it follows from Eqs. (5a) and (9) that in the present approximation we have the fixed boundary condition at the SN interface:

$$F_N = \frac{\Delta}{|\omega|} \exp(-i\varphi/2), \quad 0 \leq x \leq W_1, \quad y = 0. \quad (13)$$

#### Solution of the Usadel equations in the normal film.

The solution of the boundary value problem given by Eqs. (1), (5g), (9), (12), and (13), which determines the spatial distribution of superconducting correlations in the normal film, has the form

$$F_N(x, y) = \frac{4 \Delta \exp(-i\varphi/2)}{\pi |\omega|} \times \sum_{m=0}^{\infty} \frac{\cosh[\zeta_m(y - d_N)/\xi_N] \sin(k_m x/\xi_N)}{q_m \cosh(\zeta_m d_N/\xi_N)}, \quad (14)$$

$$q_m = 2m + 1, \quad k_m = \frac{\pi \xi_N}{2 W_1} q_m, \quad \zeta_m = \sqrt{|\omega| + k_m^2}. \quad (15)$$

Owing to Eqs. (12) and (13), this solution is independent of the form of the boundary conditions, by which the solutions in the regions 2, 4 and 1, 5 match. One can easily find from Eq. (14) the coordinate depen-

dence of the Green's functions at the interface of normal and ferromagnetic layers ( $0 \leq x \leq W_1, y = d_N$ ):

$$F_N(x, d_N) = \frac{4\Delta \exp(-i\varphi/2)}{\pi|\omega|} \times \sum_{m=0}^{\infty} \frac{\sin(k_m x / \xi_N)}{q_m \cosh(\zeta_m d_N / \xi_N)}, \quad (16)$$

which allows turning to the solution of the equations in the ferromagnetic films.

**Solution of the Usadel equations in the ferromagnetic film.** The boundary value problem specified by Eqs. (2), (5e), and (5h) in the region  $0 \leq x \leq W_1, d_N \leq y \leq d_N + d_F$  is closed by the conditions

$$F_F(x, d_N) = F_N(x), \quad (17)$$

$$\xi_F \frac{\partial}{\partial x} F_F = 0, \quad d_N \leq y \leq d_N + d_F \quad (18)$$

and has the solution

$$F_F(x, y) = \frac{\Delta \exp\left(\frac{i\varphi}{2}\right) \sinh[\sqrt{\tilde{\Omega}}(y - d_N) / \xi_F]}{|\omega| \sqrt{\tilde{\Omega}} \gamma_{BF} \cosh[\sqrt{\tilde{\Omega}} d_F / \xi_F]} + \frac{2\Delta \exp\left(-\frac{i\varphi}{2}\right)}{\pi^2} \times \sum_{s=-\infty}^{\infty} \sum_{m=0}^{\infty} \frac{\cosh[p_s(y - d_N - d_F) / \xi_F] \cos(k_s x / \xi_N)}{Z_{m,s} \cosh(p_s d_F / \xi_F) \cosh(p_s d_N / \xi_N)}, \quad (19)$$

$$k_s = \frac{\pi \xi_N}{W_1} s, \quad p_s = \sqrt{\tilde{\Omega} + k_s^2},$$

$$Z_{m,s} = \left[ \left(m + \frac{1}{2}\right)^2 - s^2 \right].$$

Substituting the function  $F_{F,\omega}(x, d_N)$  given by Eq. (19) and its derivative with respect to the coordinate  $y$  at  $y = d_N$  into Eq. (3) for the superconducting current density in the region  $I$  ( $0 \leq x \leq W_1$ ), we find the sinusoidal dependence  $J_S(\varphi) = J_c \sin \varphi$  with the critical current density  $J_{c1}$  given by

$$\frac{e R_{BF} \mathcal{A}_{BF} J_{c1}}{T} = \text{Re} \sum_{\omega, m=0}^{\infty} \frac{8\Delta^2 \sin(k_m x / \xi_N)}{\omega^2 q_m \cosh(\zeta_m d_N / \xi_N) \cosh(\sqrt{\tilde{\Omega}} d_F / \xi_F)}. \quad (20)$$

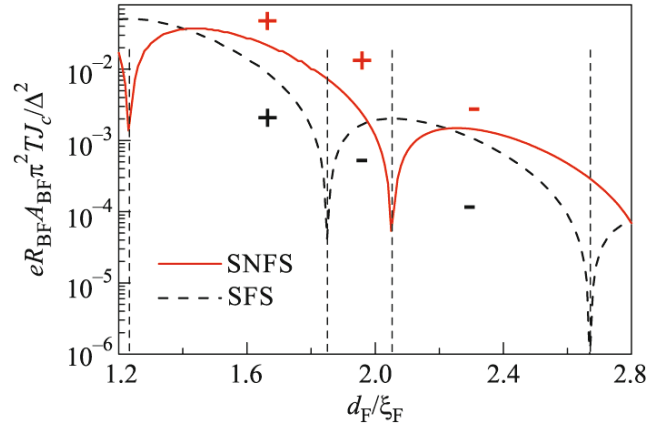


**Fig. 2.** (Color online) Critical current densities  $J_{c1}$  and  $J_{c5}$  of the SNFS and SFS segments of the SF–NFS Josephson junction, respectively, shown in Fig. 1 versus the thickness of the ferromagnetic film calculated with the use of Eqs. (20) and (21).

The boundary value problem in the region 5 ( $-W_2 \leq x \leq -d_F$ ) has the simple solution [30, 31]

$$F_F(x, y) = p_- \cosh\left[\frac{\sqrt{\tilde{\Omega}}(y - d_F)}{\xi_F}\right] + p_+ \cosh\left(\frac{\sqrt{\tilde{\Omega}} y}{\xi_F}\right),$$

$$p_{\pm} = \frac{\Delta}{\gamma_{BF} \sqrt{\tilde{\Omega}} |\omega| \sinh[\sqrt{\tilde{\Omega}} d_F / \xi_F]} \exp(\pm i\varphi/2).$$

Substitution of this solution into Eq. (3) for the supercurrent also leads to the sinusoidal dependence  $J_S(\varphi)$  with the critical current density  $J_{c5}$  given by

$$\frac{e R_{BF} \mathcal{A}_{BF} J_{c5}}{T} = \text{Re} \sum_{\omega=0}^{\infty} \frac{4\pi\Delta^2}{\gamma_{BF} \sqrt{\tilde{\Omega}} \omega^2 \sinh(\sqrt{\tilde{\Omega}} d_F / \xi_F)}. \quad (21)$$

In the regions 3 and 4 of the ferromagnetic film (see Fig. 1), the projection of the supercurrent density on the  $x$  axis is zero, since in the present approximation  $F_N = 0$  at  $x = 0, 0 \leq y \leq d_N$ , and the projection on the  $y$  axis is much less than  $J_S$  in the regions 1 and 5. This allows setting  $J_S = 0$  in the regions 2–4 without loss of generality.

Figure 2 shows the dependences  $J_{c1}(d_F)$  and  $J_{c5}(d_F)$  computed with the parameters  $T/T_c = 0.5, h = 30, \gamma_{BF} = 0.6, d_N/\xi_N = 0.2,$  and  $\xi_N/W_1 = 0.2$  corresponding to the typical experimental situation [22].

As follows from these curves, the critical current densities  $J_{c1}$  and  $J_{c5}$  in the segments 1 and 5 can have the same (positive or negative) or opposite signs depending on the thickness of the ferromagnetic layer. The respective distributions computed for the F-layer

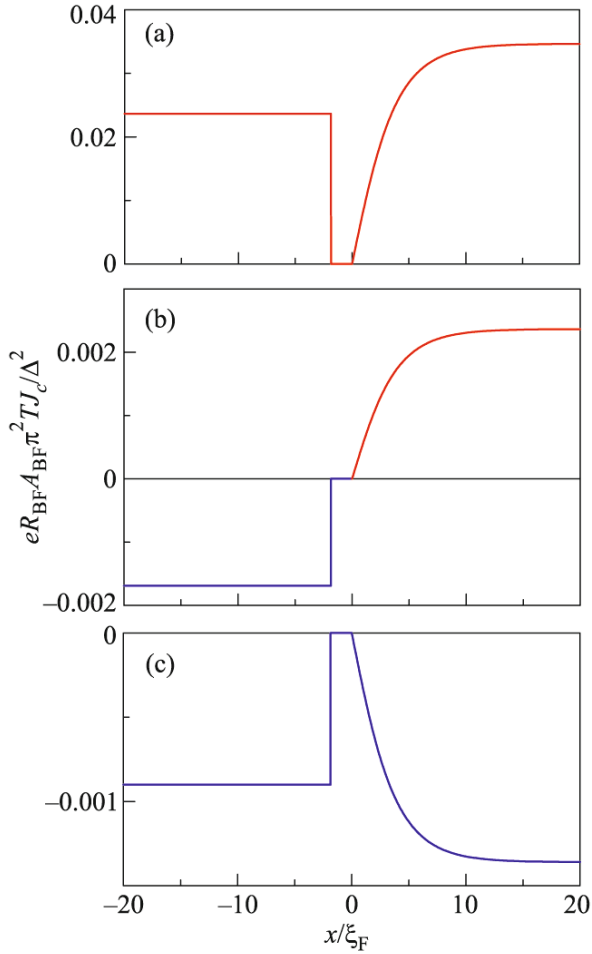


**Fig. 3.** (Color online) Critical current density versus the coordinate  $x$  near the step of the normal layer calculated for the ferromagnetic layer thickness  $d_F/\xi_F =$  (a) 1.51, (b) 1.96, and (c) 2.34.

thicknesses  $d_F/\xi_F = 1.51, 1.96,$  and  $2.34$  are exemplified in Fig. 3. In the thickness range of  $1.23 \leq d_F/\xi_F \leq 1.85$ , the SF–NFS structure is a Josephson 0 junction with a supercurrent density inhomogeneously distributed along the  $x$  axis. The ground state of this junction corresponds to the phase difference  $\varphi = 0$  of the order parameters of the electrodes. At the thicknesses  $2.05 \leq d_F/\xi_F \leq 2.67$ , we have an inhomogeneous  $\pi$  junction with the ground state corresponding to  $\varphi = \pi$ . Finally, in the range of  $1.85 < d_F/\xi_F < 2.05$ , the ground state of the junction in the case of interest of low widths  $W_1 + W_2 \ll \lambda_j$  (compared to the Josephson penetration depth  $\lambda_j$  of the magnetic field) depends considerably on the relation between the products  $J_{c1}W_1$  and  $J_{c5}W_2$  and can correspond to  $\varphi = 0, \pi$ , or some intermediate value in the range of  $0 \leq \varphi \leq \pi$  [32–34]. In this case, the critical current of the junction depends on the angle  $\theta$  between the magnetization of the ferromagnetic film and the direction separating the SFS and SNFS segments of the SFS–SNFS structure.

**Critical current of SFS–SNFS Josephson junctions.** To prove the above statement, we consider for simplicity the structure with a square cross section with the side length  $W = W_1 + W_2 = \lambda_j$  and set  $W_1 = W_2$ . To calculate its critical current as a function of the magnetization rotation angle in the contact plane (the  $xz$ ) plane in Fig. 1), one has to solve the two-dimensional sine-Gordon equation

$$\varphi_{tt} - \varphi_{xx} - \varphi_{zz} + J_c(x) \sin \varphi = -\alpha \varphi_t + j - \eta_x - \eta_z. \quad (22)$$

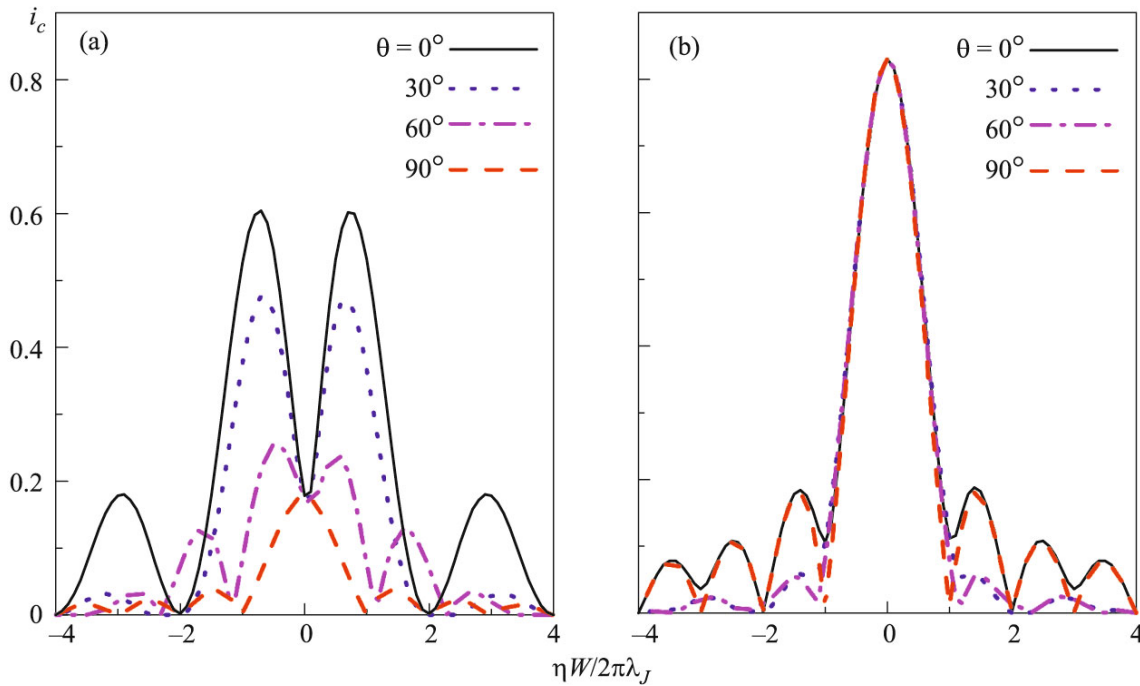
Here, the spatial coordinates  $x$  and  $z$  and the time  $t$  are normalized to  $\lambda_j$  and to the inverse plasma frequency  $\omega_p^{-1}$ , respectively ( $\omega_p = \sqrt{2\pi I_c/C\Phi_0}$ , where  $C$  is the capacitance of the junction), and  $\alpha = \omega_p/\omega_c$  is the damping constant, where  $\omega_c = 2\pi I_c R_n/\Phi_0$ . The critical current density  $J_c(x)$  and the bias current density  $j$  are normalized to the critical current density  $J_{c1}$  of the SNFS segment. The magnetization vector  $\mathbf{M} = (M_x, 0, M_z)$  is represented in Eq. (22) by its components  $\eta_x$  and  $\eta_z$  with the normalization  $\eta = 2\pi\mu_0|\mathbf{M}|\Lambda\lambda_j/\Phi_0$ , where  $\mu_0$  is the vacuum permeability and  $\Lambda$  is the magnetic thickness of the junction.

Figure 4 presents the magnetization dependence of the critical current  $I_c$  calculated for the ferromagnetic layer thicknesses lying in the ranges of  $1.85 \leq d_F/\xi_F \leq 2.05$  and  $1.23 \leq d_F/\xi_F \leq 1.85$ . In the first interval, the critical current density of the segment  $I$  in Fig. 1 is nonnegative,  $J_{c1} \geq 0$ , at the chosen parameters, whereas the SFS segment appears in the  $\pi$  state, i.e., it exhibits a negative critical current density  $J_{c5}$ . Its absolute value is  $0.66J_{c1}$ . In the second interval, both  $J_{c1}$  and  $J_{c5}$  are positive and, as in the previous case,  $J_{c5} = 0.66J_{c1}$ .

As is seen, the character of the curves in the first interval of the thickness  $d_F$  depends considerably on the angle  $\theta$  between the  $z$  axis and the magnetization vector  $\mathbf{M}$ . At  $\theta = 90^\circ$ , the dependence  $I_c(\eta)$  is a nearly Fraunhofer waveform typical of pointlike Josephson junctions [35]. With a decrease in  $\theta$ , the dependence  $I_c(\eta)$  transforms and has a minimum at  $\theta = 0^\circ$ ,  $\eta = 0$ , whereas the critical current increases sharply at  $\eta \approx 1$ .

In the second interval of thicknesses, transformation of the dependence  $I_c(\eta)$  with the angle  $\theta$  is insignificant.

Thus, our calculations actually proved that introduction of a spatial inhomogeneity to the weak-link region of the Josephson junction containing just one ferromagnetic layer leads to the formation of a superconducting spin valve of a new type. The magnitude of the critical current in this structure is determined by the orientation of the magnetization vector of the ferromagnetic film with respect to the direction separating the SFS and SNFS segments of the SF–NFS junction (the  $z$  axis in Fig. 1). Such a spin valve can appear in two states with substantially different critical currents. These states correspond to mutually orthogonal



**Fig. 4.** (Color online) Critical current of the structure under investigation versus the magnetization of the ferromagnetic layer for various angles between the magnetization and the  $z$  axis in the  $(xz)$  plane (see Fig. 1). The structure is a square in the junction plane with the side length  $W = \lambda_J$  ( $W_1 = W_2$ ). The ratio of the critical current densities in the segments is  $J_{c5}/J_{c1} =$  (a)  $-0.66$  and (b)  $0.66$ .

directions of the vector  $\mathbf{M}$ , which allows switching the valve by applying mutually orthogonal external magnetic fields. Maintenance of these states does not require external energy sources. The SF–NFS Josephson junction can be used as a control element of SIs–F/NF–S structures in the development of superconducting memory units [36].

It should be mentioned that the characteristic voltage of the proposed SIs–F/NF–S junction is close to  $V_c$  of the SIsFS Josephson junctions. Actually, the presence of the additional normal layer weakly affects  $I_c$  of its s–F/NF–S part owing to a small thickness of the normal film ( $d_N \ll \xi_N$ ) and a considerable difference between  $\xi_N$  and the lateral dimensions  $W$  of the structure. The only mechanism of the additional suppression of the critical current in the s–F/NF–S junction is a possible difference between the absolute values of the critical current of its sFS and sNFS segments. Such a suppression is on the order of the ratio of these absolute values and can be diminished by choosing proper layer thicknesses. Thus, the proposed SIs–F/NF–S valve can be a convenient solution of the contradiction formulated at the beginning of this work.

We are grateful to V.V. Ryazanov, V.V. Bol’ginov, O.A. Mukhanov, and I.I. Vernik for the discussion of the results. This work was supported in part by the Ministry of Education and Science of the Russian Federation (project nos. RFMEFI61614X0011 and

14Y26.31.0007 and the Program for the Promotion of Competitiveness of the Kazan Federal University among the World-Leading Scientific Educational Centers), by the Council of the President of the Russian Federation for Support of Young Scientists and Leading Scientific Schools (project no. MK-1841.2014.2), by the Russian Foundation for Basic Research (project nos. 14-02-90018-bel\_a, 14-02-31002-mol\_a, and 15-32-20362-mol\_a\_ved), by the Dynasty Foundation, by the Dutch Foundation for Fundamental Research on Matter, and the Council of the President of the Russian Federation for Support of Young Scientists and Leading Scientific Schools.

## REFERENCES

1. A. A. Golubov, M. Yu. Kupriyanov, and E. Il’ichev, *Rev. Mod. Phys.* **76**, 411 (2004).
2. A. I. Buzdin, *Rev. Mod. Phys.* **77**, 935 (2005).
3. F. S. Bergeret, A. F. Volkov, and K. B. Efetov, *Rev. Mod. Phys.* **77**, 1321 (2005).
4. S. Oh, D. Youm, and M. Beasley, *Appl. Phys. Lett.* **71**, 2376 (1997).
5. R. Held, J. Xu, A. Schmehl, C. W. Schneider, J. Manhart, and M. Beasley, *Appl. Phys. Lett.* **89**, 163509 (2006).
6. S. V. Bakurskiy, N. V. Klenov, I. I. Soloviev, V. V. Bol’ginov, V. V. Ryazanov, I. I. Vernik, O. A. Mukhanov, M. Yu. Kupriyanov, and A. A. Golubov, *Appl. Phys. Lett.* **102**, 192603 (2013).

7. C. Bell, G. Burnell, C. W. Leung, E. J. Tarte, D.-J. Kang, and M. G. Blamire, *Appl. Phys. Lett.* **84**, 1153 (2004).
8. F. S. Bergeret, A. F. Volkov, and K. B. Efetov, *Rev. Mod. Phys.* **77**, 1321 (2005).
9. J. W. A. Robinson, J. D. S. Witt, and M. G. Blamire, *Science* **329**, 59 (2010).
10. D. Sprungmann, K. Westerholt, H. Zabel, M. Weides, and H. Kohlstedt, *Phys. Rev. B* **82**, 060505(R) (2010).
11. G. B. Halasz, M. G. Blamire, and J. W. A. Robinson, *Phys. Rev. B* **84**, 024517 (2011).
12. B. Baek, W. H. Rippard, S. P. Benz, S. E. Russek, and P. D. Dresselhaus, *Nature Commun.* **5**, 3888 (2014).
13. A. Iovan, T. Golod, and V. M. Krasnov, arXiv:1405.4754 (2014).
14. J. W. A. Robinson, N. Banerjee, and M. G. Blamire, *Phys. Rev. B* **89**, 104505 (2014).
15. M. Alidoust and K. Halterman, *Phys. Rev. B* **89**, 195111 (2014).
16. B. M. Niedzielski, S. G. Diesch, E. C. Gingrich, Y. Wang, R. Loloee, W. P. Pratt, and N. O. Birge, *IEEE Trans. Appl. Supercond.* **24**, 1800307 (2014).
17. O. A. Mukhanov, *IEEE Trans. Appl. Supercond.* **21**, 760 (2011).
18. V. V. Ryazanov, V. V. Bol'ginov, D. S. Sobanin, I. V. Vernik, S. K. Tolpygo, A. M. Kadin, and O. A. Mukhanov, *Phys. Proc.* **36**, 35 (2012).
19. T. I. Larkin, V. V. Bol'ginov, V. S. Stolyarov, V. V. Ryazanov, I. V. Vernik, S. K. Tolpygo, and O. A. Mukhanov, *Appl. Phys. Lett.* **100**, 222601 (2012).
20. I. V. Vernik, V. V. Bol'ginov, S. V. Bakurskiy, A. A. Golubov, M. Yu. Kupriyanov, V. V. Ryazanov, and O. A. Mukhanov, *IEEE Trans. Appl. Supercond.* **23**, 1701208 (2013).
21. S. V. Bakurskiy, N. V. Klenov, I. I. Soloviev, M. Yu. Kupriyanov, and A. A. Golubov, *Phys. Rev. B* **88**, 144519 (2013).
22. S. M. Frolov, D. J. van Harlingen, V. V. Bolginov, V. A. Oboznov, and V. V. Ryazanov, *Phys. Rev. B* **74**, 020503(R) (2006).
23. M. Weides, C. Schindler, and H. Kohlstedt, *J. Appl. Phys.* **101**, 063902 (2007).
24. J. Pfeiffer, M. Kemmler, D. Koelle, R. Kleiner, E. Goldobin, M. Weides, A. Feofanov, J. Lisenfeld, and A. Ustinov, *Phys. Rev. B* **77**, 214506 (2008).
25. C. Gürlich, S. Scharinger, M. Weides, H. Kohlstedt, R. G. Mints, E. Goldobin, D. Koelle, and R. Kleiner, *Phys. Rev. B* **81**, 094502 (2010).
26. M. Kemmler, M. Weides, M. Weiler, M. Opel, S. T. B. Goennenwein, A. S. Vasenko, A. A. Golubov, H. Kohlstedt, D. Koelle, R. Kleiner, and E. Goldobin, *Phys. Rev. B* **81**, 054522 (2010).
27. N. Pugach, M. Kupriyanov, A. Vedyayev, C. Lacroix, E. Goldobin, D. Koelle, R. Kleiner, and A. Sidorenko, *Phys. Rev. B* **80**, 134516 (2009).
28. K. D. Usadel, *Phys. Rev. Lett.* **25**, 507 (1970).
29. M. Yu. Kupriyanov and V. F. Lukichev, *Sov. Phys. JETP* **67**, 1163 (1988).
30. A. A. Golubov, M. Y. Kupriyanov, and Y. V. Fominov, *JETP Lett.* **81**, 335 (2005).
31. A. Buzdin, *JETP Lett.* **78**, 583 (2003).
32. A. Buzdin and A. E. Koshelev, *Phys. Rev. B* **67**, 220504(R) (2003).
33. E. Goldobin, H. Sickinger, M. Weides, N. Ruppelt, H. Kohlstedt, R. Kleiner, and D. Koelle, *Appl. Phys. Lett.* **102**, 242602 (2013).
34. A. Lipman, R. G. Mints, R. Kleiner, D. Koelle, and E. Goldobin, *Phys. Rev. B* **90**, 184502 (2014).
35. K. K. Likharev, *Rev. Mod. Phys.* **51**, 101 (1979).
36. I. I. Soloviev, N. V. Klenov, S. V. Bakurskiy, V. V. Bol'ginov, V. V. Ryazanov, M. Yu. Kupriyanov, and A. A. Golubov, *Appl. Phys. Lett.* **105**, 242601 (2014).

*Translated by A. Safonov*